

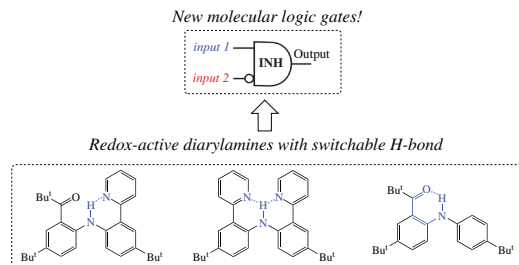
## Diarylamines with switchable intramolecular H-bonding: a new approach to molecular logic gates

Oleg A. Levitskiy, Yuri K. Grishin and Tatiana V. Magdesieva\*

Department of Chemistry, M. V. Lomonosov Moscow State University, 119991 Moscow, Russian Federation.  
E-mail: [tvm@org.chem.msu.ru](mailto:tvm@org.chem.msu.ru)

DOI: 10.1016/j.mencom.2024.02.029

New *ortho*-substituted diarylamines prone to different types of the intramolecular H-bonding (IMHB) were obtained. In-depth NMR, IR and voltammetry study allowed selecting the amine that demonstrates stable reversible switching of the IMHB bond under the external stimuli, which can be used for the logic gate construction.

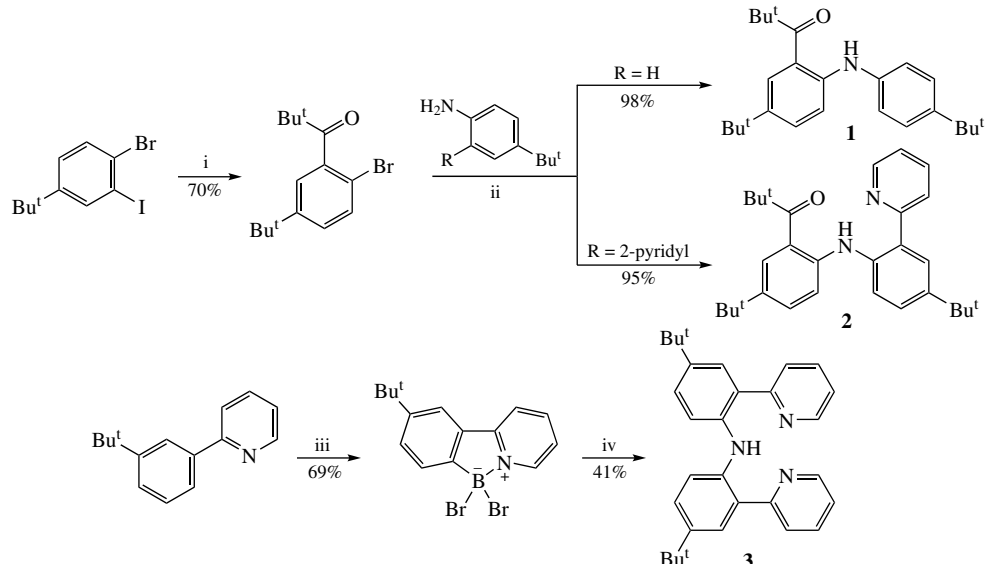


**Keywords:** intramolecular hydrogen bond, molecular logic gates, diarylamines, molecular switches, anodic oxidation.

Hydrogen bond is one of the most important types of non-covalent interactions. Its energy can be widely varied, providing an extra stabilization of 1–40 kcal mol<sup>-1</sup> to the molecular systems involved.<sup>1,2</sup> Intramolecular H-bonding (IMHB) is of special interest. It can be easily destroyed by conformational changes<sup>3</sup> or by altering the pH value of the medium, providing new elegant synthetic routes<sup>4,5</sup> or giving rise to various types of molecular switches,<sup>6–8</sup> logic gates,<sup>9–12</sup> etc. Functioning of natural systems is also often based on such interactions.<sup>13</sup>

Diarylamines are convenient models for implementation of switchable intramolecular H-bonding. *ortho*-Modification of the aromatic rings with the appropriate substituents in the close vicinity to the NH group creates prerequisites for the reversible tuning of the amino group functionality (its nucleophilicity, oxidation potential value, basicity, etc.).

Herein, molecular design, synthesis and in-depth study of three new *ortho*-substituted diarylamines **1–3** (Scheme 1) prone to different types of the IMHB will be discussed. A convenient research algorithm based on the combination of spectral and electrochemical methods was proposed. IR and <sup>1</sup>H NMR studies make it possible to establish the presence of an intramolecular H-bond; <sup>1</sup>H NMR spectra measured in different solvents clarify a possibility for switching between the inter- and intramolecular H-bonding in response to environmental changes. The voltammetry study allows the H-bond to be classified into types and to distinguish between the competing resonance-assisted (RAHB)<sup>14</sup> and ‘common’ hydrogen bonding. The compounds with three different types of intramolecular H-bonding are of interest as the convenient models for the fundamental study of the hydrogen bond as a tool for switching and controlling



**Scheme 1** Reagents and conditions: *i*, Pr<sup>i</sup>MgCl, THF, -78 °C, then CuCl (0.5 equiv.), -30 °C, then Bu<sup>t</sup>C(O)Cl, -30 → +20 °C; *ii*, Pd<sub>2</sub>(dba)<sub>3</sub> (5 mol%), dppf (6 mol%), Bu<sup>t</sup>ONa (1.1 equiv.), PhMe, 110 °C; *iii*, BBBr<sub>3</sub> (3 equiv.), Et<sub>3</sub>N (1 equiv.), CH<sub>2</sub>Cl<sub>2</sub>; *iv*, Me<sub>2</sub>CH(CH<sub>2</sub>)<sub>2</sub>ONO, CuI (5 mol%), Et<sub>3</sub>N, EtOH.

molecular systems. One of the new amines was tested as a working material in a model INH (inhibit) logic gate and showed promising results.

Amines **1**, **2** were obtained in almost quantitative yield using the Buchwald–Hartwig amination. The precursor, 2-pivaloyl-4-*tert*-butylphenyl bromide, also has not been described previously. It was synthesized *via* the trans-metallation of the Grignard reagent using CuCl; the thus formed aryl cuprate was acylated with pivaloyl chloride<sup>15</sup> giving the target bromide in practical 70% yield. Direct Friedel–Crafts acylation of the starting bromide is not applicable since the Lewis acid would destroy pivaloyl chloride and initiate the *tert*-butyl group migration thus making the process unselective. Symmetrical diarylamine **3**<sup>16</sup> was obtained *via* the electrophilic *ortho*-borylation of the aromatic ring<sup>17</sup> followed by the reaction with isoamyl nitrite.<sup>18</sup>

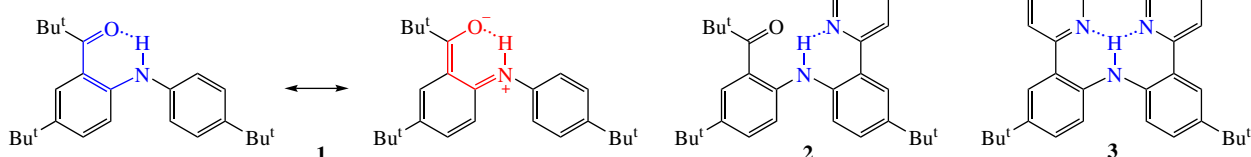
The intramolecular H-bond formation in amines **1–3** was studied using the <sup>1</sup>H NMR and IR spectroscopy (Table 1). The signals for the NH protons measured in CDCl<sub>3</sub> (which is not capable of strong IMHB) were significantly downfield shifted as compared to the free NH group in CDCl<sub>3</sub> in all cases; the chemical shifts were 8.88 ppm (for **1**), 10.49 ppm (for **2**), and 10.73 ppm (for **3**). This testifies in favor of the intramolecular H-bond formation. The conclusion was also supported by the low  $\nu(\text{NH})$  values: for **1–3**, they fall within the 3220–3280 cm<sup>−1</sup> range (see Table 1; for comparison: the vibration frequency of the free N–H bond in diarylamines is commonly much higher,<sup>15</sup> *viz.* 3370–3460 cm<sup>−1</sup>). Thus, both methods provided a direct evidence for the strong intramolecular H-bonding in compounds **1–3**.

The <sup>1</sup>H NMR spectra were also recorded in DMSO-d<sub>6</sub> which is known as a good H-bond acceptor.<sup>19</sup> The  $\delta(\text{NH})$  chemical shifts stayed almost unchanged for amines **2** and **3** (see Table 1). Thus, we can conclude that the IMHB is strong enough and reserved in DMSO. In contrast, the chemical shift of the NH group in **1** is significantly upfield shifted in DMSO as compared to the sample in CDCl<sub>3</sub> indicating that the NH bond is removed of the carbonyl group plane. Thus, the IMHB in amine **1** is weak and loses the competition with the intermolecular H-bond with DMSO molecules.

The detailed analysis of the <sup>1</sup>H NMR spectrum shows that the structure of amine **3** is symmetrical; this testifies in favor of the IMHB bonding between the NH and the both pyridyl substituents (Scheme 2). The DFT calculations (PBEh-3c) also confirmed the three-center H bond formation. Non-covalent interactions within the optimized structure of **3** can be visualized using the approach proposed previously.<sup>20</sup> The IMHB between the NH and

**Table 1** The NH chemical shifts, the NH bond stretching frequencies, peak potentials for amines **1–3** oxidation (measured at 0.1 V s<sup>−1</sup> scan rate at Pt in 0.1 M solution of Bu<sub>4</sub>NBF<sub>4</sub> in MeCN vs. Ag/AgCl, KCl<sub>sat</sub>) and corresponding half-wave potentials (measured at a scan rate where reversible response was observed).

Amine	$\delta_{\text{NH}}^{\text{CDCl}_3}$ /ppm	$\delta_{\text{NH}}^{\text{DMSO}}$ /ppm	$\nu_{\text{NH}}$ /cm <sup>−1</sup>	$E_{\text{pa}}^{(1)}$ ( $E_{1/2}$ )/V	$E_{\text{pa}}^{(2)}$ ; $E_{\text{pa}}^{(3)}$ /V
<b>1</b>	8.88	7.89	3270	1.13 (1.04)	—
<b>2</b>	10.49	10.49	3221	0.90 (0.91)	1.24
<b>3</b>	10.73	10.97	3273	0.85 (0.86)	1.01; 1.32



**Scheme 2**

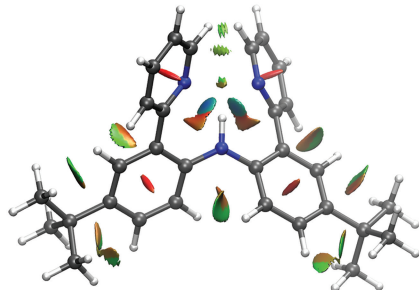


**Figure 1** Low-gradient isosurfaces with low densities visualizing noncovalent interactions in amine **3**.

the both pyridyl groups is shown in Figure 1 as two blue-colored areas.

Electrochemical study helps to shed more light on the IMHB nature in amines **1–3** since it provides information about the electron density at the amino group. Voltammetry investigation was performed at a Pt disk electrode in MeCN using Bu<sub>4</sub>NBF<sub>4</sub> as a supporting electrolyte. Oxidation of all amines was irreversible at low potential scan rates (see Online Supplementary Materials); the reversible oxidation was detected only at a scan rate of 50 V<sup>−1</sup> that prevents the chemical follow-up step. That allowed us to determine the formal potential values as well (see Table 1).

As it has been shown previously,<sup>15</sup> the *ortho*-located pyridyl group in the close vicinity to the NH group of the diaryl amine facilitates its oxidation due to the partial donation of the pyridines' lone pair to the amino group *via* strong IMHB bonding. However, that is not the case in amine **1**. Its oxidation is impeded as compared to the model bis(4-*tert*-butylphenyl)-amine ( $E_p = 0.93$  V *vs.* Ag/AgCl, KCl<sub>sat</sub>), in spite of the IMHB that was reliably confirmed using the spectral methods (see above). The reason is that the IMHB between the amino group and the carbonyl or the pyridyl substituents are of a principally different nature. The pyridyl group is a strong H-bond acceptor due to the high-lying nitrogen lone pair, whereas the carbonyl group can act as the H-bond acceptor only in the case of the resonance-assisted H-bonding<sup>14</sup> (see Scheme 2).

In amine **2**, the IMHB is 'switched' from the carbonyl group to the stronger H bond acceptor, *i.e.*, to the pyridyl fragment. This structural modification causes the significant downfield shift of the NH signal in <sup>1</sup>H NMR (in both CDCl<sub>3</sub> and DMSO, see Table 1) and a decrease in the vibration frequency of the N–H bond in the IR spectrum.

For amines **2**, **3**, a series of oxidation peaks can be observed in the anodic region. The second oxidation peak is kinetically related to the first one and attributed to the oxidation of the protonated form of the amine: the radical cations formed in the first oxidation step lose protons, the latter protonate the starting amine, in line with the previously reported data.<sup>21,22</sup>

Notably, protonation of the Py group in **2** destroys the IMHB; consequently, the second oxidation potential is significantly shifted anodically (for 0.34 V). In contrast, the IMHB in **3** is still reserved after protonation of only one Py group (though it becomes a two-centered H bond); therefore, the difference in two consecutive oxidations in **3** is low (0.16 V). Protonation of the both Py groups in **3** destroys the IMHB resulting in the

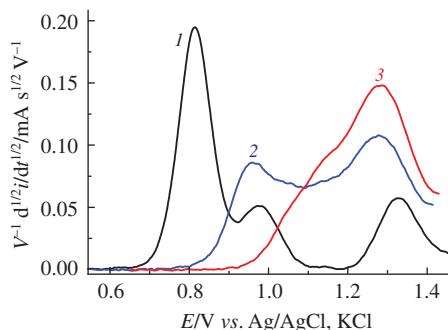


**Figure 2** Semi-differential voltammogram for amine **3** (MeCN, 0.1 M  $\text{Bu}_4\text{NBF}_4$ , Pt) with varying amounts of TsOH added (curve *1*: no acid; curve *2*: with 1 equiv. of TsOH; curve *3*: with 2 equiv. of TsOH).

significant anodic shift of the third oxidation peak (0.31 V). It is worth mentioning that the first oxidation potential of **3** is almost equal to that for its mono-pyridyl substituted analog previously reported<sup>15</sup> ( $E_{\text{pa}} = 0.85$  V). This means that two pyridyl groups in **3** create the same excess of the electron density on the N atom of the amino group as one *ortho*-pyridyl substituent. Thus, protonation of the pyridyl group dramatically shifts the oxidation potential of the amine **3** only if the IMHB is completely destroyed.

The assignment of the consecutive oxidation peaks in the voltammogram of **3** was additionally confirmed by the experiment with the external acid (*p*-toluenesulfonic acid TsOH) additives. The first oxidation peak (corresponding to the non-protonated amine) disappeared after addition of 1 equiv. of TsOH to the solution of **3**, whereas the current corresponding to the two other peaks was increased (Figure 2). When 2 equiv. of TsOH were added, the IMHB in **3** was completely destroyed and the only one (the most anodic) peak can be observed in the voltammogram.

The molecules exhibiting strong intramolecular interactions are of interest as possible candidates for implementation of molecular switching under an external stimuli. The well-pronounced reversible changes in the voltammetric behavior of amine **3** after addition of the acid discussed above allows considering **3** as a possible candidate for the logic gate creation with the recruitment of the voltammetric control.

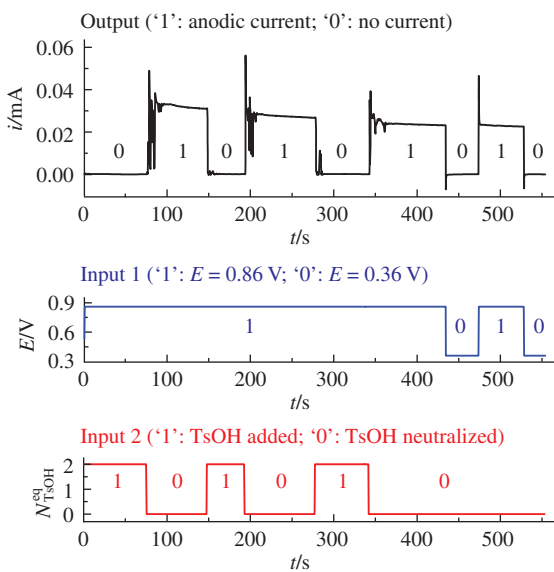
Logic gates are defined as devices that make the input signals transform to specific output signals by Boolean logic operations.

Molecular logic gates usually require compounds to respond to one, two, or more external stimuli, which include chemical and biological effects (such as metal ions, anions, acids, bases, DNA, enzymes, viruses, *etc.*), as well as physical effects (such as light, heat, and electricity) and then convert the input signals to the output signals in logic systems by binary Boolean logic rules. The common output signals involve UV absorption, fluorescence emission, circular dichroism, electrochemistry, *etc.*<sup>23</sup> Combinational molecular gates allow a single molecule to process complex operations. The most widely used are YES, NOT, OR, NOR, AND, and INHIBIT gates.<sup>24</sup>

A possible logic diagram illustrating the operating principles of the INH (*inhibit*) logic gate is shown in Figure 3 (right). It is driven by two inequivalent inputs; the signal at the first input induces the appearance of the output signal only if the second (prohibiting) input gives no signal (is switched off).

In our case, the two inputs are the electrode potential and the acid/base additive. The logic variable ‘0’ at the first input corresponds to the applied potential which is less anodic than the first oxidation peak of amine **3**, whereas the logic variable ‘1’ stems for the potential region where oxidation of the neutral and the mono-protonated amine **3** takes place (in our experiments,  $E = 0.86$  V was chosen). As for the second input, logic ‘1’ corresponds to the acid (2 equiv.) added to the amine solution (both pyridyl groups are protonated) whereas logic ‘0’ means that no acid is added (or it is neutralized by a base), therefore the IMHB is reserved.

To test the idea, the model logic element was constructed. The output signal was an anodic current at a rotating disk platinum working electrode operating at 200 rpm rotation rate immersed into the solution of amine **3** in MeCN with  $\text{Bu}_4\text{NBF}_4$  as a supporting electrolyte. The working electrode potential was switched between 0.86 V (the first oxidation peak) and 0.36 V (no oxidation), corresponding to logic variables ‘1’ and ‘0’ at input 1, respectively. The acetonitrile solution of TsOH was added by portions containing 2 equiv. of the acid or neutralized by the equal amount of a base (the 2,6-lutidine solution). The anodic current at the working electrode appeared in accordance with the INH logic gate truth table (see Figure 3). The acid plays a role of a prohibitory input: in the absence of the acid, the current can be switched on/off solely by the potential changing, while no influence of the potential switching on the current is observed when 2 equiv. of the acid was added.



INH truth table		
Input 1	Input 2	Output
0	0	0
1	0	1
0	1	0
1	1	0

Input 1: ‘1’:  $E = 0.86$  V; ‘0’:  $E = 0.36$  V

Input 2: ‘1’: TsOH added; ‘0’: TsOH neutralized

Output: Anodic current

**Figure 3** Experimental testing of the model molecular logic gate based on amine **3** (left figure; black curve corresponds to the output signal which is the anodic current at the RDE as a function of the signals at two inputs. The modular behavior of the input signals is indicated by the blue and red curves), the INH logic gate truth table and the corresponding logic scheme (right).

To conclude, new amines described herein are convenient models for the deeper understanding of the H-bonding as a possible tool for switching and controlling molecular systems. The spectral and electrochemical study revealed the different types of the IMHB in amines **1–3**. In **1**, the resonance-assisted IMHB is formed. The *ortho*-positioned carbonyl group in **1** decreases the electron density on the N atom of the amino group due to the ‘push-pull’ conjugation; consequently, it becomes a strong acceptor of the H-bond. In **2**, this type of the IMHB loses competition with a more basic pyridyl group. In **3**, a symmetrical three-center IMHB is formed involving both *ortho*-pyridyl substituents and the NH group. Depending on the structural type of the IMHB the amino group is involved in, the electron density on the N atom varies significantly. These differences can be voltametrically detected by changes in the oxidation potential values.

We demonstrated that reversible switching of the intramolecular H-bond in amine **3** under the external stimuli can be used for the logic gate construction. Switching of the oxidation current (the output) under combined action of two inputs (H<sup>+</sup> and potential) makes a single molecule capable of performing logic operations. It should be emphasized that the majority of stimuli-responsive smart systems are based on complex molecular/supramolecular and polymeric architectures to achieve the desired function (see, *e.g.*, refs. 25, 26). Thus, simple and available amine **3** demonstrating stable and reversible output seems rather prospective.

This work was supported by Russian Science Foundation (grant no. 22-73-00040). The NMR part of this work was supported by M. V. Lomonosov Moscow State University Program of Development.

#### Online Supplementary Materials

Supplementary data associated with this article can be found in the online version at doi: 10.1016/j.mencom.2024.02.029.

#### References

- 1 G. A. Jeffrey, *An Introduction to Hydrogen Bonding*, Oxford University Press, 1997.
- 2 G. Gilli and P. Gilli, *The Nature of the Hydrogen Bond*, Oxford University Press, 2009.

- 3 E. G. Kononova, I. A. Solonina, M. N. Rodnikova and E. V. Shirokova, *Mendeleev Commun.*, 2022, **32**, 837.
- 4 *Hydrogen Bonding in Organic Synthesis*, ed. P. M. Pihko, Wiley, 2009.
- 5 *Non-covalent Interactions in the Synthesis and Design of New Compounds*, eds. A. M. Maharramov, K. T. Mahmudov, M. N. Kopylovich and A. J. L. Pombeiro, Wiley, 2016.
- 6 J. D. Harris, M. J. Moran and I. Aprahamian, *Proc. Natl. Acad. Sci. USA*, 2018, **115**, 9414.
- 7 G. Hum, S. J. I. Phang, H. C. Ong, F. León, S. Quek, Y. X. J. Khoo, C. Li, Y. Li, J. K. Clegg, J. Díaz, M. C. Stuparu and F. García, *J. Am. Chem. Soc.*, 2023, **145**, 12475.
- 8 O. Jin, D. Fu, Y. Ge, J. Wei and J. Guo, *New J. Chem.*, 2015, **39**, 254.
- 9 X. Cao, X. Zeng, L. Mu, Y. Chen, R.-X. Wang, Y.-Q. Zhang, J.-X. Zhang and G. Wei, *Sens. Actuators, B*, 2013, **177**, 493.
- 10 N. Busschaert, C. Caltagirone, W. van Rossom and P. A. Gale, *Chem. Rev.*, 2015, **115**, 8038.
- 11 A. P. de Silva and S. Uchiyama, *Nat. Nanotechnol.*, 2007, **2**, 399.
- 12 R. Bhaskar, N. Mageswari, D. Sankar and G. G. V. Kumar, *Mater. Lett.*, 2022, **327**, 133040.
- 13 K. Ariga, *Int. J. Mol. Sci.*, 2022, **23**, 3577.
- 14 K. T. Mahmudov and A. J. L. Pombeiro, *Chem. – Eur. J.*, 2016, **22**, 16356.
- 15 O. A. Levitskiy, I. A. Klimchuk, Y. K. Grishin, V. A. Roznyatovsky, B. N. Tarasevich and T. V. Magdesieva, *Synthesis*, 2022, **54**, 1601.
- 16 I. V. Prolubshikov, O. A. Levitskiy, S. G. Dorofeev, Y. K. Grishin, K. A. Lyssenko and T. V. Magdesieva, *Dyes Pigm.*, 2023, **218**, 111525.
- 17 N. Ishida, T. Moriya, T. Goya and M. Murakami, *J. Org. Chem.*, 2010, **75**, 8709.
- 18 O. A. Levitskiy and T. V. Magdesieva, *Org. Lett.*, 2019, **21**, 10028.
- 19 M. H. Abraham, *Chem. Soc. Rev.*, 1993, **22**, 73.
- 20 E. R. Johnson, S. Keinan, P. Mori-Sánchez, J. Contreras-García, A. J. Cohen and W. Yang, *J. Am. Chem. Soc.*, 2010, **132**, 6498.
- 21 D. Serve, *Electrochim. Acta*, 1976, **21**, 1171.
- 22 O. A. Levitskiy, D. A. Dulov, O. M. Nikitin, A. V. Bogdanov, D. B. Eremin, K. A. Paseshnichenko and T. V. Magdesieva, *ChemElectroChem*, 2018, **5**, 3391.
- 23 B. Li, D. Zhao, F. Wang, X. Zhang, W. Li and L. Fan, *Dalton Trans.*, 2021, **50**, 14967.
- 24 C.-Y. Yao, H.-Y. Lin, H. S. N. Crory and A. P. de Silva, *Mol. Syst. Des. Eng.*, 2020, **5**, 1325.
- 25 X. Zhang, L. Chen, K. H. Lim, S. Gonuguntla, K. W. Lim, D. Pranantyo, W. P. Yong, W. J. T. Yam, Z. Low, W. J. Teo, H. P. Nien, Q. W. Loh and S. Soh, *Adv. Mater.*, 2019, **31**, 1804540.
- 26 Q. Yu, B. Aguila, J. Gao, P. Xu, Q. Chen, J. Yan, D. Xing, Y. Chen, P. Cheng, Z. Zhang and S. Ma, *Chem. – Eur. J.*, 2019, **25**, 5611.

Received: 5th December 2023; Com. 23/7332